

A Fully Integrated Planar Toroidal Inductor with a Micromachined Nickel–Iron Magnetic Bar

Chong H. Ahn, *Member, IEEE*, Yong J. Kim, and Mark G. Allen, *Member, IEEE*

Abstract—A fully integrated toroidal inductor is realized on a silicon wafer by using a multilevel metalization technique to fabricate a wrapped coil wound around a micromachined bar of high-permeability magnetic material. In particular, efforts are made to minimize the coil resistance by using thick conductor lines and electroplated vias. In this structure, a 30 μm thick nickel–iron permalloy magnetic core is wrapped with 40 μm thick multilevel copper conductor lines, constructing a conventional toroidal inductor in planar shape. A closed magnetic circuit (i.e., toroidal) in this inductive component is adopted, where magnetic core bar and wrapped conductor lines are tightly interlinked, so that leakage flux and electromagnetic interference are minimized. For an inductor size of 4 mm \times 1 mm \times 130 μm thickness having 33 turns of multilevel coils, the achieved inductance is approximately 0.4–0.1 μH at 1 kHz–1 MHz, corresponding to a core permeability of approximately 800. The measured dc resistance of the conductor lines is approximately 0.3 Ω . Since this inductive component shows favorable magnetic characteristics as well as electrical properties, it is potentially very useful as a basic inductive component in applications for magnetic microsensors, microactuators, and micromagnetic power devices such as a dc/dc converter.

Index Terms—Fully integrated, planar, toroidal inductor, micromachined component, nickel-iron, microactuator, micromachining technique, dc/dc converter.

I. INTRODUCTION

RECENTLY the demands for new planar integrated inductors [1]–[4] that have high inductance and Q-factor have greatly increased for applications such as magnetic microactuators [5]–[8] and integrated micromagnetic power devices [3], [9]. Unfortunately, integration of an inductive component has been the major obstacle in the fabrication of fully integrated, miniaturized magnetic actuators or devices. To demonstrate the feasibility of a planar toroidal inductor, a toroidal inductive component was fabricated in a hybrid fashion by manually wrapping coils around a bar-type magnetic film core by Soohoo [1]. It was verified from this demonstrated structure that the introduction of a permalloy thin film increased the inductance value by a factor of 1000 when compared with an air core [1]. However, the fabrication of this three-dimensional

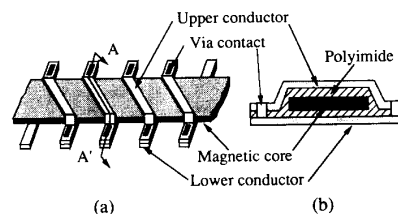


Fig. 1. Schematic diagram of the planar bar-type inductive component: (a) schematic view, (b) A – A' cut view.

inductive structure in a planar geometry has been understood to be an extremely difficult task. To fabricate this inductor on a planar substrate, quasi-three-dimensional micromachining techniques that are compatible with IC processes are required.

In this paper, a planar toroidal inductive component (hereafter referred to as a bar-type inductor), consisting of multilevel conductor coils wrapped around a bar of high permeability magnetic material, is realized on a silicon wafer using metal interconnection techniques. In this structure, the interconnected metal coils wrap around the magnetic core bar. The bar-type inductive component is considered one of the more promising inductive components for micromagnetic power device applications, since its geometrical characteristics can meet most of the required conditions of a basic inductive component for micromagnetic applications [10].

An air-core inductor consisting of wrapped solenoid coils on a silicon substrate was fabricated previously by Kawahito [2] for the application of highly sensitive magnetic sensors. However, the obtained electrical parameters are unsuitable for micromagnetic power device applications due to limitations on the achievable conductor thickness (and therefore the current carrying capability of the inductor) imposed by the fabrication process. In this paper, however, a new technique is adopted to overcome these limitations using planarization with polyimides and inserting a magnetic bar core in place of the air core. The proposed inductor structure is depicted in Fig. 1, where the geometry can be thought of as analogous to the conventional toroidal inductor.

The metal interconnections used to construct the wrapping coils usually include metal via contacts. These via contacts are another obstacle in the practical applications of this component since they may have a relatively high contact resistance that causes a specific heat dissipation in the via contacts. In achieving a high inductance value, if more turns of solenoid coils are required, more via contacts are added, increasing the total coil resistance. Evaporated metal deposition techniques

Manuscript received October 8, 1993; revised May 1994. This work was supported in part by the National Science Foundation under Grant ECS-9117074. This paper was presented at the 7th International Conference on Solid-State Sensors and Actuators, Yokohama, Japan, June 7–10, 1993.

C. H. Ahn is with the IBM Thomas J. Watson Research Center, Yorktown Heights, NY 10598 USA.

Y. J. Kim and M. G. Allen are with the School of Electrical and Computer Engineering and the Microelectronics Research Center, Georgia Institute of Technology, Atlanta, GA 30332 USA.

IEEE Log Number 9403537.

TABLE I
COMPOSITION OF THE NICKEL-IRON AND COPPER ELECTROPLATING SOLUTIONS

Nickel-iron permalloy		Copper	
Component	Quantity (g/l)	Component	Quantity
$NiSO_4 \cdot 6H_2O$	200	$CuSO_4 \cdot 5H_2O$	1200 (g/l)
$FeSO_4 \cdot 7H_2O$	8	H_2SO_4	100 (ml/l)
$NiCl_2 \cdot 6H_2O$	5		
H_3BO_3	25		
Saccharin	3		

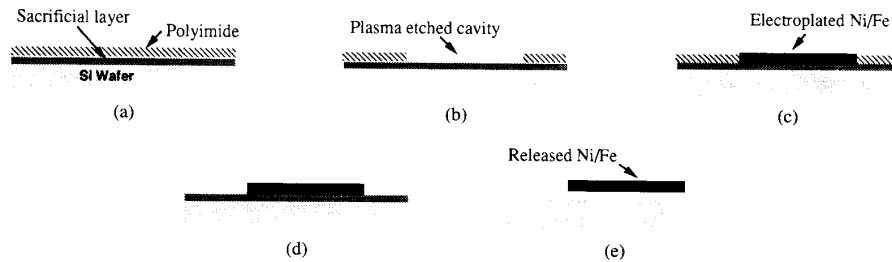


Fig. 2. Fabrication sequence of the test samples for the *in situ* measurement of magnetic properties: (a) sacrificial layer and polyimide deposition; (b) cavity etching; (c) nickel/iron plating; (d) polyimide etching; (e) nickel/iron release.

limit the achievable thickness of a deposited metal. These techniques usually cause a high metal contact resistance at the via contacts due to metal oxide or surface contamination resulting from subsequent fabrication processes [11]–[13]. As a result, when a high current is applied to the conductor coils, heat is generated locally at the via contacts due to their high resistance, resulting in a potential instability problem in this inductive component.

To solve this problem, in this paper we have used an electroplating technique to fabricate the conductor lines and the vias, because the electroplated metal contacts usually have a low metal contact resistance [12]–[13]. If the resistance per via contact can be reduced to the several $m\Omega$ range using the electroplating technique, the restriction caused by the high via contact resistance might be removed.

In realizing this component, particular efforts have been made to minimize the coil resistance by increasing the thickness of the conductor lines and using electroplated vias. An additional feature of this inductor is that a closed (i.e., toroidal) magnetic circuit is achieved, minimizing the leakage flux and electromagnetic interference, and increasing the inductance value and the Q-factor.

II. MAGNETIC MATERIAL AND IN SITU CHARACTERIZATION

In designing a planar inductive component, magnetic material properties measured from bulk-type magnetic samples may not be useful since the magnetic properties may depend on film geometry, thickness, and size. Thus, before designing a planar inductor, the magnetic properties of the bar-type core should be understood. In measuring the magnetic properties of the magnetic film used for a micromagnetic structure, it is

important to remember that the magnetic properties of interest must be measured *in situ*; that is, on as-deposited films.

Among the available soft magnetic materials, nickel-iron permalloy has been used as a promising magnetic material in a variety of magnetic film applications since it has favorable magnetic [14]–[15] as well as mechanical [16] properties. In particular, the composition of Ni/Fe nickel (81%)/iron (19%) film can meet the requirements as a magnetic material for magnetic microactuator applications, because this composition can simultaneously achieve maximum permeability, minimum coercive force, minimum anisotropy field, and maximum mechanical hardness. Nickel/iron nickel (81%)/iron (19%) permalloy can be deposited using either evaporation or electroplating, but in this research the electroplating technique is adopted due to the cost advantage in making a film of several tens of microns. For the electroplating, a plating bath was built using the compositions shown in Table I [14]–[15].

Test samples were then prepared using surface micromachining techniques such that they could meet the *in situ* measurement requirement. To prepare test samples, the fabrication sequence, which is similar to the fabrication steps described later in this paper, is shown in Fig. 2. This fabrication was performed using the same fabrication mask sets that are to be used in the fabrication of actual magnetic components. Thus, the prepared test samples have exactly the same sizes and the same geometries as the magnetic films used in the micromachined magnetic components. The geometry of test samples that were prepared for *in situ* measurement in this research was a bar-type film.

The measurements of material $B-H$ curves were obtained from magnetization (or moment) versus applied field curves

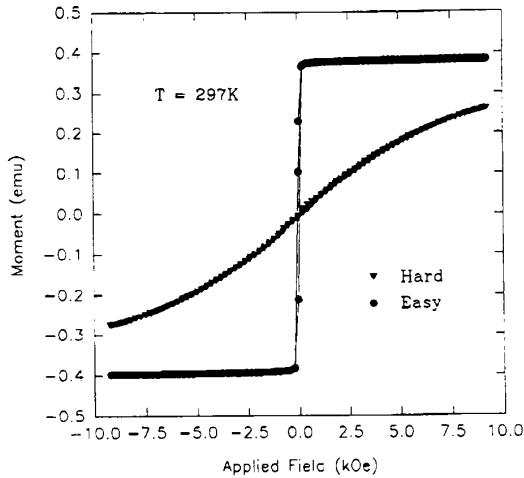


Fig. 3. Magnetization (emu (SI unit)) as a function of applied dc field using the low field measurements for the bar-type core.

which are obtained using a vibrating sample magnetometer (Model 4500, Lake Shore Cryotronics, Inc.). Fig. 3 illustrates the results from the low-field measurements for the bar-type film. From the $B - H$ values evaluated from the values shown in Fig. 3, the bar-type magnetic core is saturated at approximately 0.8 (T) and the evaluated relative permeability μ_r shows 800 at the linear region. It should be emphasized that the above calculation assumes zero demagnetization effect. Note that the relative permeability and flux saturation at high frequencies may have different values from those obtained at low frequencies in this section.

In order to measure the relative permeability of the magnetic core film, another approach using an indirect measurement technique was performed, using a toroidal inductor fabricated in a hybrid fashion. First, a magnetic core ring was prepared using the same surface micromachined procedures described in Fig. 2, where the inner and the outer diameters of the core ring were 0.15 cm and 0.32 cm, respectively, producing the width of the core ring of 0.085 cm. The thickness of the electroplated core ring was 50 μm . To construct a toroidal inductor in a hybrid fashion, enamel insulated copper conductor of 125 μm in diameter was manually wrapped around the core ring. The achieved number of coil turns was 21. The photograph of the toroidal inductor in a hybrid fashion mounted on a chip carrier is shown in Fig. 4. This toroidal inductor was mounted on chip and then tested by using an impedance analyzer. The measured inductance was 2.5 μH at low frequencies of approximately 1 KHz.

The calculation of inductance for a toroidal inductor is very simple and more or less straightforward, as reported earlier [1]. The inductance L of the toroidal inductor structure is expressed as

$$L = \frac{\mu_0 \mu_r N^2 A_c}{l_c} \quad (1)$$

where A_c is the cross sectional area of the magnetic core ring, l_c is the length of the closed magnetic core ring at

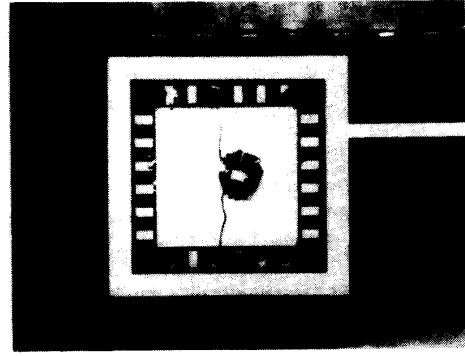


Fig. 4. The photograph of the toroidal inductor in a hybrid fashion mounted on a chip carrier.

the average diameter, and μ_0 and μ_r are the permeability of the vacuum and the relative permeability of the magnetic core, respectively. If the measured inductance value and the geometry of the toroidal inductor are known, the relative permeability μ_r can be evaluated from (1). In the toroidal inductor fabricated with the magnetic core ring, $L = 2.5 \mu\text{H}$, $A_c = 850 \mu\text{m} \times 50 \mu\text{m}$, $N = 21$ turns, and $l_c = \pi \times 0.235$ cm; thus the μ_r evaluated for the magnetic core ring (this ring is analogous to the bar-type core in comparison) is approximately 780. This value is almost comparable to the permeability of 800 obtained from the vibrating sample magnetometer described earlier in this section.

III. STRUCTURE DESIGN

As shown in Fig. 1, this component is composed of the magnetic core bar and the multilevel metal interconnections, whose geometry has a similar structure to a conventional wrapped inductor except for its planar shape. In order to accomplish the wrapping function of the conductor coils on a planar surface, the patterned lower conductor lines are interconnected to the upper conductor lines through metal vias, wrapping around a magnetic core bar and constructing a quasi-three-dimensional structure. To compose a closed magnetic circuit between the coils and the magnetic cores, the magnetic core bars are placed on top of the lower conductor lines after the lower conductor lines are patterned and insulated, and then the coils are completed, wrapping around the magnetic cores and constructing an interlinkage with the magnetic cores.

As mentioned earlier, a planar inductive component should achieve an inductance value as high as possible, keeping the conductor resistance as low as possible to achieve a high Q-factor and to reduce the heat loss [17]. In this structure, the achievable inductance values depend on both the wrapping coil turns and the magnetic reluctance of the magnetic core bar, where the magnetic reluctance is determined from the dimension and the permeability of the core bar. For a given area, the width of the conductor lines affects both the number of turns and the resistance of the conductors; thus its width should be chosen so as to achieve a high Q-factor.

However, the major difficulty in realizing this structure in a planar shape comes from its fabrication difficulty. In the design

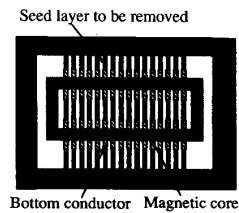


Fig. 5. Tie bar-type seed layer, which is to be removed upon completion of fabrication after serving as a plating seed layer.

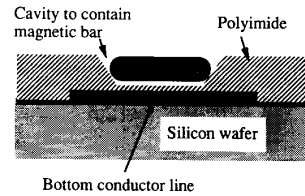


Fig. 6. Cavity that is etched through polyimide to contain the magnetic core bar.

of this structure, the fabrication difficulties encountered are considered first, and then a modified design of this structure is followed to overcome the fabrication obstacles.

Among several obstacles encountered in fabricating this inductive component, the major difficulty comes from the fabrication of thick wrapping coils which have a low conductor resistance. Electroplating is a favorable technique for deposition of the thick metal conductor, but electroplating usually requires a plating seed layer that must be removed after completing the fabrication of the structure. Consequently, the seed layer used for the lower conductor lines should remain to serve as the plating seed layer for the via and the upper conductor plating until the component fabrication is completed. The seed layer must then be removed, or all of the coils will be shorted together. Unfortunately, the seed layer is now difficult to remove, as it is at the bottom of the structure. Simple blanket etching to expose the seed layer will not work, as the magnetic core bar placed on the top of the lower conductors serves as a mask to prevent complete exposure of the seed layer.

To solve this problem, a tie bar-type seed layer as depicted in Fig. 5 is introduced. The tie bars can serve as the electroplating seed layer for the conductor lines and vias until the fabrication is completed. When the fabrication of this component is finished, the edges of the tie bars can be exposed using a blanket plasma etch and then removed, ensuring the electrical isolation of the coils.

Another difficulty in the fabrication comes from the need to fabricate a thick magnetic core bar (for low magnetic reluctance) which should be placed on the top of the insulated lower conductor lines. The relatively high aspect ratio of the magnetic core causes a serious difficulty in patterning the conductor vias and the upper conductor lines, due to poor planarization of the surface. If a cavity is made to contain the magnetic bar so that the magnetic bar is recessed, planarization of the surface for subsequent processing can be achieved. In this paper, a cavity to contain the magnetic core bar is introduced in an insulating layer using a dry etching technique. The magnetic core can be inserted in this insulated cavity without destroying the planarization of the surface, as shown in Fig. 6. The size of designed inductor is $4 \text{ mm} \times 1 \text{ mm}$, having 33 turns of conductor coils, where the width of conductor line and bar-core are $80 \text{ }\mu\text{m}$ and $300 \text{ }\mu\text{m}$, respectively.

IV. FABRICATION

A brief fabrication process of this component is shown in Fig. 7. The process starts with an oxidized ($0.6 \text{ }\mu\text{m}$) 2-

in $\langle 100 \rangle$ silicon wafer as a substrate. Onto this substrate, chromium (500 \AA)/copper (2000 \AA)/chromium (700 \AA) layers were deposited using electron-beam evaporation to form an electroplating seed layer. This seed layer was patterned to form the tie bars to be removed after serving as the seed layer for the conductor plating. Polyimide (Dupont PI-2611) was then spun on the wafer to build electroplating molds for the bottom conductor lines. Four coats were cast to obtain a $40 \text{ }\mu\text{m}$ thick polyimide film. Each coat was spun by continuous two-step spin speeds (700 rpm for 10 s , 3000 rpm for 4 s) and soft baked for 10 min at $120 \text{ }^\circ\text{C}$ prior to the application of the next coat. After the deposition of all coats, the polyimide was cured at $350 \text{ }^\circ\text{C}$ for 1 h in nitrogen, yielding an after-cure thickness of $40 \text{ }\mu\text{m}$. Holes that contained lower conductor lines of $40 \text{ }\mu\text{m}$ thickness were etched in this polyimide using an O_2 (100%) plasma etch and an aluminum hard mask until the chromium/copper/chromium seed layer was exposed. The copper conductors were plated through the defined molds using standard electroplating technique [11]–[13] and the copper plating solution described in Table I.

Polyimide (PI-2611) was multi-spincoated and cured to construct a cavity $40 \text{ }\mu\text{m}$ in depth to contain a magnetic core bar. As mentioned in the previous section, the cavity to contain the magnetic core bar was dry etched using the same process described earlier. In order to achieve a smooth surface at the steep edge of the cavity that ensures the smooth connection of the plating seed layer, polyimide (PI-2611) was spincoated at 3000 rpm and hard-cured using the same conditions described above. The same seed layer (chromium/copper/chromium) used for the plating of the lower conductor lines was deposited again for the magnetic core plating.

Nickel/iron nickel (81%)/iron (19%) was then plated using the same processes used in fabricating the magnetic core described in the previous section. Upon completion of the electroplating, the chromium/copper/chromium seed layer was wet etched using a potassium-ferricyanide based chromium etching solution and a cupric-sulfate based copper etching solution, respectively.

To insulate the conductor lines and to replanarize the surface, more polyimide was deposited in multiple coats (as described above). Via holes were then dry etched through the polyimide layer using 100% oxygen plasma and an aluminum hard mask. Upon completion of the via etch, the aluminum hard mask was removed. Because the surface of the lower conductor strips was exposed to the oxygen plasma during dry etching, the surface of the copper was oxidized. To remove the oxide film, the exposed area of the lower conductors was

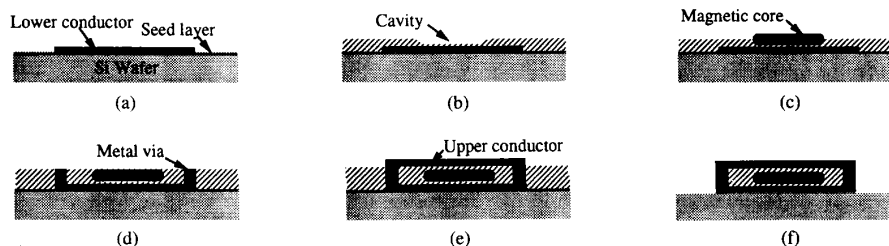


Fig. 7. Fabrication steps of the bar-type inductive component: (a) patterning of bottom conductors; (b) dry etching of cavity to contain magnetic core; (c) magnetic core plating; (d) via conductor plating; (e) patterning of top conductors; (f) removal of seed layer.

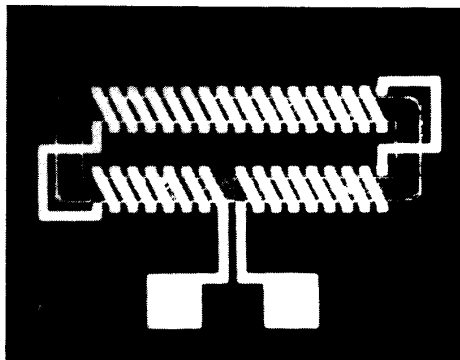


Fig. 8. Photomicrograph of the fabricated bar-type inductor.

etched in a sulfuric acid (2%) solution for 10 s. Plating contact was then made to the seed layer of the lower conductors, and the metal vias were filled with plated copper using the copper electroplating bath and conditions described previously. Upon completion of the electroplating, a copper (2000 Å)/chromium (700 Å) layer was deposited again, and the copper plating mold was formed using 40 μm thick photosensitive polyimide (Prohimide 349, OCG Microelectronic Materials) [8], [10], [11]. The upper conductor lines were plated through the defined molds using the same plating conditions described above. After removing the photosensitive polyimide in a KOH-based solution, the plating seed layer for the top conductors was wet etched.

To remove the chromium/copper/chromium plating seed layer in the shape of the tie bars located underneath the fabricated component, the insulating polyimide was dry etched to the bottom using an aluminum mask and the chromium/copper/chromium was then wet etched. Fig. 8 shows the photomicrograph of the fully fabricated device. The scanning electron micrographs of the structure are shown in Fig. 9, which were taken after dry etching of the polyimide. At the completion of fabrication, samples were diced into chips for bonding and test, as shown in Fig. 10.

V. MODELING

The geometry of the bar-type inductor depicted in Fig. 1 can be analogous to the conventional toroidal inductor. Thus, the calculation of inductance for the bar-type structure is very simple and more or less straightforward, as explained in

the magnetic material section as well as reported earlier [1]. The inductance L of the bar-type inductor structure shown in Fig. 1 was expressed in (1). Equation (1) assumes that the relative permeability of the insulating material is equal to unity. To evaluate an inductance of the designed inductor, it is useful to substitute the designed geometries and the measured permeability into (1). For $A_c = 300 \mu\text{m} \times 20 \mu\text{m}$, $l_c = 9000 \mu\text{m}$, $N = 33$ turns, and $\mu_r = 800$, the evaluated inductance value by using (1) is 0.729 μH.

The Q factor of the inductor can be expressed as

$$Q = \frac{\omega L}{R} = \frac{\omega \mu_0 \mu_r N A_c A_w}{2W \rho l_c}, \quad (2)$$

where A_w is the cross sectional area of the conductor, $2W$ is the length of coil per turn, and ρ is the resistivity of the conductor material. For $W = 600 \mu\text{m}$, $\rho = 2 \times 10^{-8} \Omega\text{-m}$, $A_w = 80 \mu\text{m} \times 38 \mu\text{m}$, and the same geometry used in the inductance calculation, the Q-factor evaluated from (3) is approximately 0.1 at 10 KHz.

From (1) and (2), it is concluded that inductance and Q-factor are linearly proportional to μ_r in the bar-type inductor as well as the conventional toroidal inductor due to the analogous structure of both inductors. Thus, the introduction of a thin-film magnetic core in the integrated inductor should improve its feasibility for IC applications. Eddy current losses in the magnetic core as well as skin depth effect in the conductor should be neglected in this calculation. This assumption should be justified since bar-type inductors fabricated using IC technology will have cores and conductor lines which have dimensions on the order of several tens of microns.

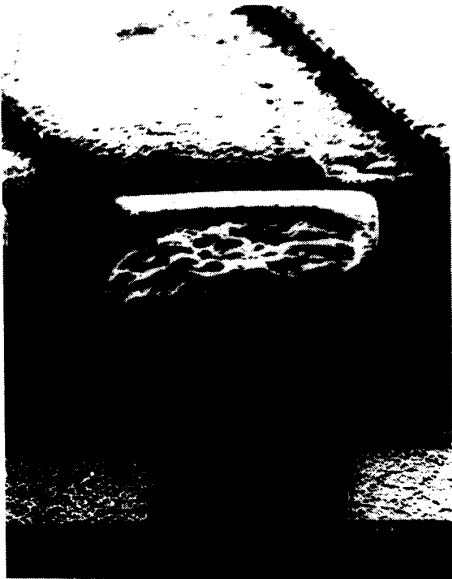
VI. EXPERIMENTAL RESULTS AND DISCUSSION

For an inductor size of 4 mm × 1 mm × 130 μm thickness having 33 turns of multilevel coils, the achieved inductance was approximately 0.4 μH at low frequencies of approximately 10 KHz, corresponding to a core permeability of 800. The variation of the inductance with frequency is shown in Fig. 11. As evaluated in the previous section, the evaluated inductance for this fabricated inductor was 0.72 μH for $\mu_r = 800$. Thus, the measured and the evaluated inductances are matched well at low frequencies.

The measured dc resistance of the conductor lines was approximately 0.3 Ω. The conductor resistance evaluated from its geometry was approximately 0.308 Ω using a literature



(a)



(b)

Fig. 9. Scanning electron micrograph of a section of the fabricated bar-type inductor: (a) inductor; (b) conductor via.

value for conductivity of plated copper [13]. Although it was difficult to measure a via contact resistance individually, it was verified from the comparison between the measured and the estimated values that the resistance of a metal via contact had an almost negligible value. Thus, as mentioned in the introduction, the electroplating technique eliminated via contact instability or high contact resistance problems potentially resulting from unfavorable metal via contacts. The evaluated and measured Q -factors at 1 MHz were approximately 4.6 and 1.5, respectively.

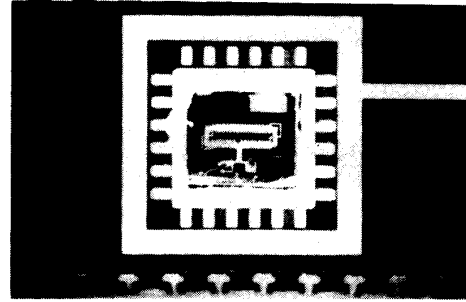


Fig. 10. Photomicrograph of the fabricated inductor mounted on the chip carrier.

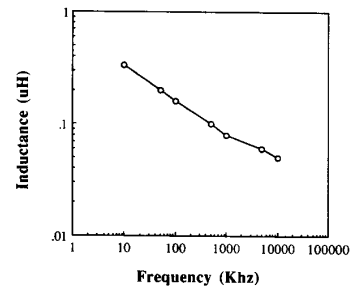


Fig. 11. Measured inductance of the fabricated inductor as a function of excitation frequency.

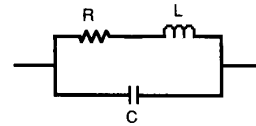


Fig. 12. Equivalent circuit of the bar-type inductor for electrical parameter evaluation.

In order to obtain the circuit parameters of the inductor, an equivalent circuit was assumed as shown in Fig. 12, and the resistance and stray capacitance of the inductor were derived from the measured impedance and phase as a function of frequency using equivalent circuit analysis. From this analysis, the stray capacitance was shown to be in the pF region, and also shown to have a negligibly small effect over the frequency ranges used. The effect of the inductance falloff at higher frequencies shown in Fig. 11 is due almost entirely to the dependence of the permeability of the nickel-iron core on frequency, and has been confirmed using other test structures.

VII. CONCLUSION

A new fully integrated bar-type inductive component has been proposed, designed, fabricated, and tested using the micromachining techniques and the metal interconnection techniques. In particular, efforts are made to minimize the coil resistance by using thick conductor lines and electroplated vias. An additional design constraint for this inductor is the use of a closed (i.e., toroidal) magnetic circuit, so that

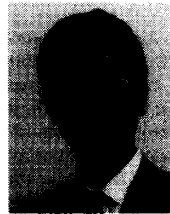
leakage flux and electromagnetic interference is minimized. For an inductor size of $4 \text{ mm} \times 1 \text{ mm} \times 130 \text{ }\mu\text{m}$ thickness having 33 turns of multilevel coils, the achieved inductance is approximately $0.4\text{--}0.1 \text{ }\mu\text{H}$ at $1 \text{ kHz--}1 \text{ MHz}$, corresponding to a core permeability of approximately 800. The measured dc resistance of the conductor lines is approximately $0.3 \text{ }\Omega$.

Since this inductive component has favorable magnetic characteristics as well as electrical properties, it is potentially very useful as a basic inductive component in applications for magnetic microsensors, microactuators, and micromagnetic power devices such as a dc/dc converter.

REFERENCES

- [1] R. F. Soohoo, "Magnetic thin film inductor for integrated circuit application," *IEEE Trans. Magn.*, vol. MAG-15, pp. 1803–1805, 1979.
- [2] S. Kawahito, Y. Sasaki, M. Ashiki, and T. Nakamura, "Micromachined solenoids for highly sensitive magnetic sensors," in *Proc. Transducers, 6th Int. Conf. Solid-State Sensors and Actuators*, pp. 1077–1080, 1991.
- [3] C. H. Ahn, Y. J. Kim, and M. G. Allen, "A fully integrated micromachined toroidal inductor with a nickel-iron magnetic core (the switched dc/dc converter application)," in *Proc. Transducers, 7th Int. Conf. Solid-State Sensors and Actuators*, pp. 70–73, 1993.
- [4] C. H. Ahn and M. G. Allen, "A new toroidal-meander type integrated inductor with a multilevel meander magnetic core," *IEEE Trans. Magn.*, vol. 30, no. 1, pp. 73–79, 1994.
- [5] B. Wagner, M. Kreutzer, and W. Benecke, "Linear and rotational magnetic micromotors fabricated using silicon technology," in *Proc. IEEE Microelectromechanical Systems Workshop*, pp. 183–189, 1992.
- [6] I. J. Busch-Vishniac, "The case for magnetically driven microactuators," *Sensors and Actuators*, vol. A, 33, pp. 207–220, 1992.
- [7] C. H. Ahn and M. G. Allen, "A fully integrated surface micromachined magnetic microactuator with a multilevel meander magnetic core," *IEEE J. Microelectromech. Syst.*, vol. 2, no. 1, pp. 15–22, 1993.
- [8] C. H. Ahn, Y. J. Kim, and M. G. Allen, "A planar variable reluctance magnetic micromotor with fully integrated stators," *IEEE J. Microelectromech. Syst.*, vol. 2, no. 4, pp. 165–173, 1993.
- [9] M. Mino, T. Yachi, A. Tago, K. Yanagisawa, and K. Sakakibara, "A new planar microtransformer for use in micro-switching converters," *IEEE Trans. Magn.*, vol. 28, no. 4, pp. 1969–1973, 1992.
- [10] C. H. Ahn, "Micromachined components as integrated inductors and magnetic microactuators," Ph.D. dissertation, Georgia Inst. of Technology, Atlanta, 1993.
- [11] K. K. Chakravorty, C. P. Chien, J. M. Cech, M. H. Tanielian, and P. L. Young, "High-density interconnection using photosensitive polyimide and electroplated copper conductor lines," *IEEE Trans. Comp., Hybrids, Manuf. Technol.*, vol. 13, no. 1, pp. 200–206, 1990.
- [12] R. Jensen, J. Cummings, and H. Vora, "Copper/polyimide materials system for high performance packaging," *IEEE Trans. Comp., Hybrids, Manuf. Technol.*, vol. 7, no. 4, pp. 384–393, 1990.
- [13] N. Iwasaki and S. Yamaguchi, "A pillar-shaped via structure in a Cu-polyimide multilayer substrate," *IEEE Trans. Comp., Hybrids, Manuf. Technol.*, vol. 13, no. 2, pp. 440–443, 1990.
- [14] M. E. Henstock and E. S. Spencer-Timms, "The composition of thin electrodeposited alloy films with special reference to nickel-iron," in *Proc. 6th Int. Metal Finishing Conf.*, pp. 179–185, 1963.

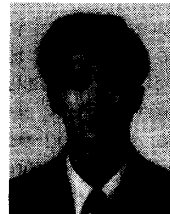
- [15] I. W. Wolf, "Electrodeposition of magnetic materials," *J. Appl. Phys.*, vol. 33, no. 3, pp. 1152–1159, 1962.
- [16] R. D. MacInnis and K. V. Gow, "Tensile strength and hardness of electrodeposited nickel-iron foil," *Plating*, pp. 135–136, 1971.
- [17] M. T. Quirke, J. J. Barrett, and M. Hayes, "Planar magnetic component technology—a review," *IEEE Trans. Comp., Hybrids, Manuf. Technol.*, vol. 15, no. 5, pp. 884–892, 1992.



Chong H. Ahn (S'90–M'91) received the B.S. degree from Inha University, Korea, in 1980, the M.S. degree from the Seoul National University, Korea, in 1983, and the Ph.D. degree from Georgia Institute of Technology, Atlanta, in 1993, all in electrical engineering.

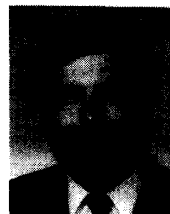
He is currently a Postdoctoral Fellow at IBM Thomas J. Watson Research Center, Yorktown Heights, NY. His research interests include the development, design, fabrication, and characterization of high aspect ratio (HAR) micro electro mechanical systems (MEMS); fully integrated microsensors and microactuators; micromachined planar inductive components; planar magnetic micromotors; integrated dc/dc converters; and integrated magnetic particle separators, using micromachining technologies.

Dr. Ahn is a member of the ASME.



Yong J. Kim received the B.S. degree from Yonsei University, Seoul, Korea, in 1987, and the M.S. degree from the University of Missouri, Columbia, in 1989, both in electrical engineering. He is now a Ph.D. candidate in the School of Electrical Engineering at Georgia Institute of Technology, Atlanta.

His research include the microactuators using magnetic components, applications of electroless plating technique in micromachining, and investigation of mechanical properties of Polyimides.



Mark G. Allen (M'89) received the B.A. degree in chemistry, the B.S.E. degree in chemical engineering, and the B.S.E. degree in electrical engineering from the University of Pennsylvania in 1984, the S.M. degree in 1986, and the Ph.D. degree in 1989, both from the Massachusetts Institute of Technology, Cambridge.

In 1989 he joined the Georgia Institute of Technology, Atlanta, where he is currently Associate Professor of Electrical and Computer Engineering.

His research interests include micromachining fabrication technology, micro-optomechanical systems, and material issues in micromachined structures and electronic packages.

Dr. Allen is a member of the editorial board of the *Journal of Micromechanics and Microengineering*.